Prime Geometry III: A Unified Action–Curvature Theory of Prime Gap Dynamics

Allen Proxmire

Abstract

Prime gaps are traditionally modeled as weakly dependent random variables of size $\Theta(\log p_n)$, governed heuristically by Cramér's model and the Hardy–Littlewood conjectures. Prime Geometry offers a complementary approach: a geometric and dynamical framework built from the algebraic identity linking three consecutive Prime Triangles,

$$(C_2 - C_1)(C_1 + C_2) = p_{n+2}^2 - p_n^2.$$

From this identity arise the geometric energy E_n, curvature K_n, and the normalized curvature

$$\chi_n = \frac{g_{n+2} - g_n}{g_n + g_{n+1}}, \qquad L_n = \chi_n^2,$$

which together define the action functional $S = \sum_n L_n$. Prime Geometry II revealed that the true prime gap sequence exhibits strong dynamical regularity: suppressed curvature relative to random permutations, long coherent curvature epochs, and a compact attractor in (χ_n, χ_{n+1})-space.

In this third paper we provide a unified action–curvature theory explaining these observations. We derive the Prime Dynamical Law governing transitions between consecutive gaps, show how the Prime Triangle identity encodes a variational principle, and provide a geometric explanation for attractor structure and curvature suppression. Large-scale computational experiments—including action minimization, perturbation stability, attractor geometry, and multi-scale curvature persistence up to one million primes—support this framework.

Prime Geometry III completes the synthesis of the algebraic foundation (PG1) and the empirical curvature dynamics (PG2) into a single geometric perspective: *the primes evolve through gap space along a low-curvature, near–least-action trajectory.*

Contents

1 Introduction

2 Prime Geometry Framework

3 Curvature and the Action Functional

4 The Prime Dynamical Law

5 The Prime Geometry Attractor

6 Predictions of the Unified Theory

7 Experimental Program

This section presents the numerical experiments supporting the action–curvature theory introduced in PG3.

7.1 Experiment A: Action Scaling

For each $N \in \{50{,}000,\ 100{,}000,\ 250{,}000,\ 500{,}000,\ 1{,}000{,}000\}$ we computed

$$S = \sum_{n=1}^{N-2} \chi_n^2,$$

and compared S_{true} with 200 random permutations of the same gap multiset.

N	S_{true}	$\mathbb{E}[S_\pi]$	$\text{Std}[S_\pi]$	Percentile
50,000	3.7164×10^4	3.8695×10^4	7.6877×10^2	1.50%
100,000	7.9151×10^4	8.2914×10^4	1.1935×10^3	$< 0.01\%$
250,000	2.1745×10^5	2.2300×10^5	1.9839×10^3	0.50%
500,000	4.4732×10^5	4.6662×10^5	3.4040×10^3	$< 0.01\%$
1,000,000	9.4165×10^5	9.7474×10^5	5.2355×10^3	$< 0.01\%$

Table 1: Experiment A: Total action S for true primes versus random permutations. True primes lie in the extreme least-action tail for all N, with the action gap increasing as N grows.

8 Experiment B: Perturbation Stability

8.1 Adjacent Swap Plot

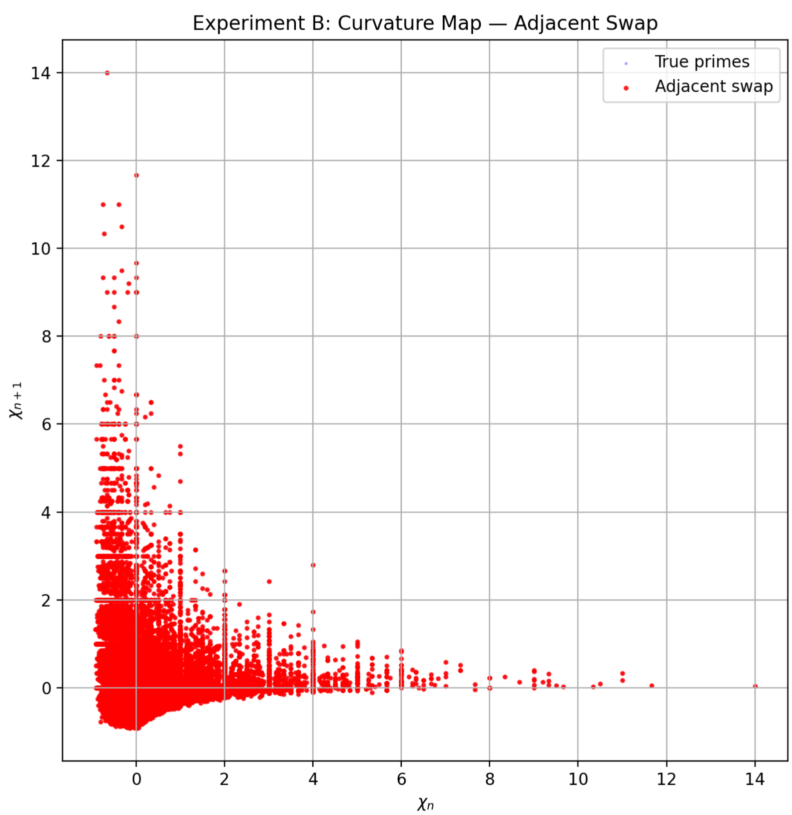

Figure 1: Experiment B (Adjacent Swap): The blue points show the true prime curvature attractor in (χ_n, χ_{n+1})-space. Red points show the effect of swapping a single adjacent pair of gaps. Even though the action increases by only $\Delta S \approx 3.9$, the perturbation ejects curvature significantly beyond the attractor boundary. This demonstrates the extreme sensitivity of curvature dynamics to gap ordering.

8.2 Local Adjustment Plot

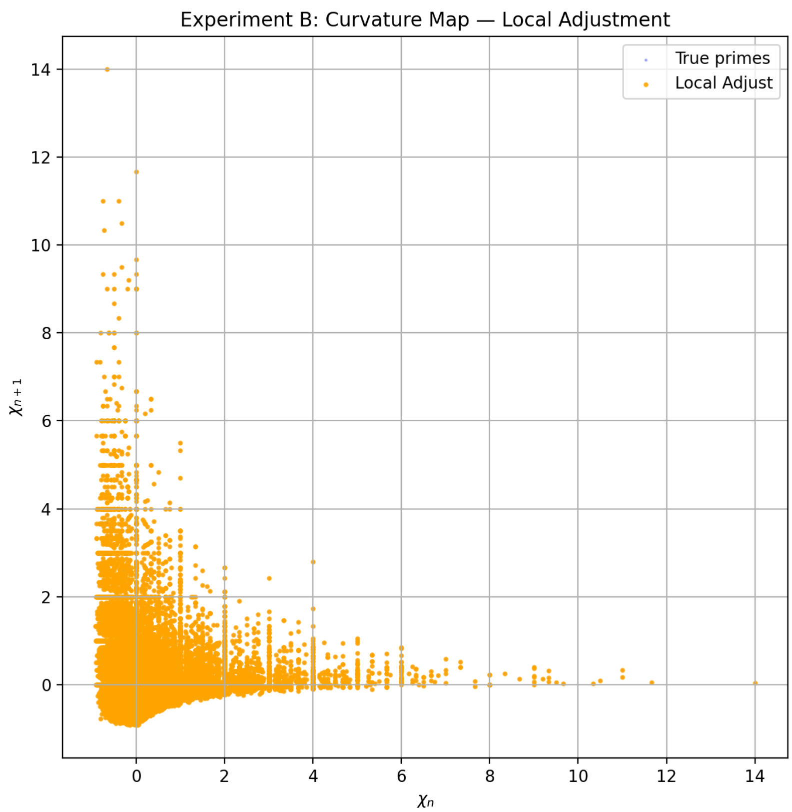

Figure 2: Experiment B (Local Adjustment): A small perturbation $g_n \mapsto g_n+5$ produces dramatic curvature spikes up to $\chi \approx 14$. The true attractor is shown in blue; the perturbed sequence in orange. Despite a tiny action change ($\Delta S \approx 1.9$), curvature escapes the entire attractor region. This shows that the attractor is defined by gap *ordering*, not by gap magnitudes alone.

8.3 Window Randomization Plot

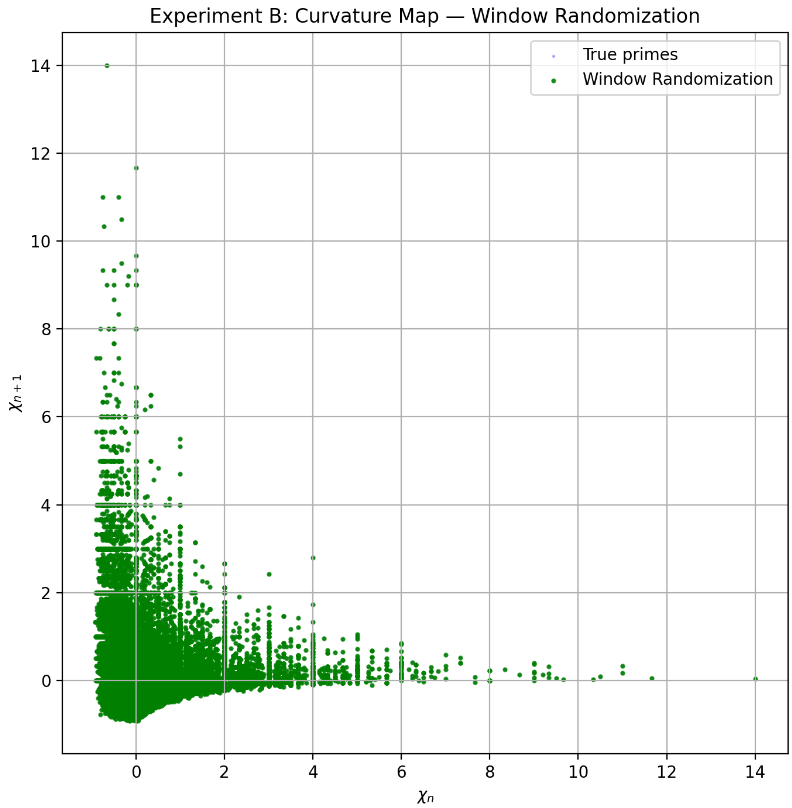

Figure 3: Experiment B (Window Randomization): Randomizing a small block of gaps breaks the fine geometric coherence of the prime curvature dynamic. The perturbed points (green) fill the entire right-hand region of the return map, destroying the attractor structure. Even this local reordering dramatically increases curvature irregularity.

9 Experiment C: Attractor Geometry

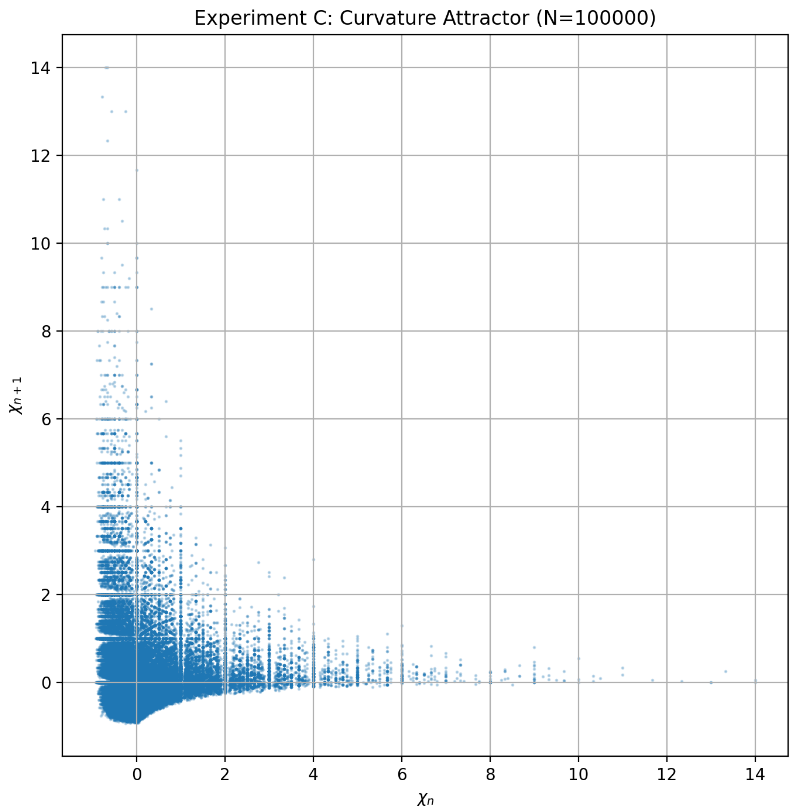

Figure 4: Experiment C: Scatter plot of the curvature attractor for $N = 100{,}000$. Almost all points lie in a compact neighborhood around $(0, 0)$, with a sharply defined boundary near radius $r \approx 14$. The attractor is nearly isotropic with mild stretching along the anti-diagonal.

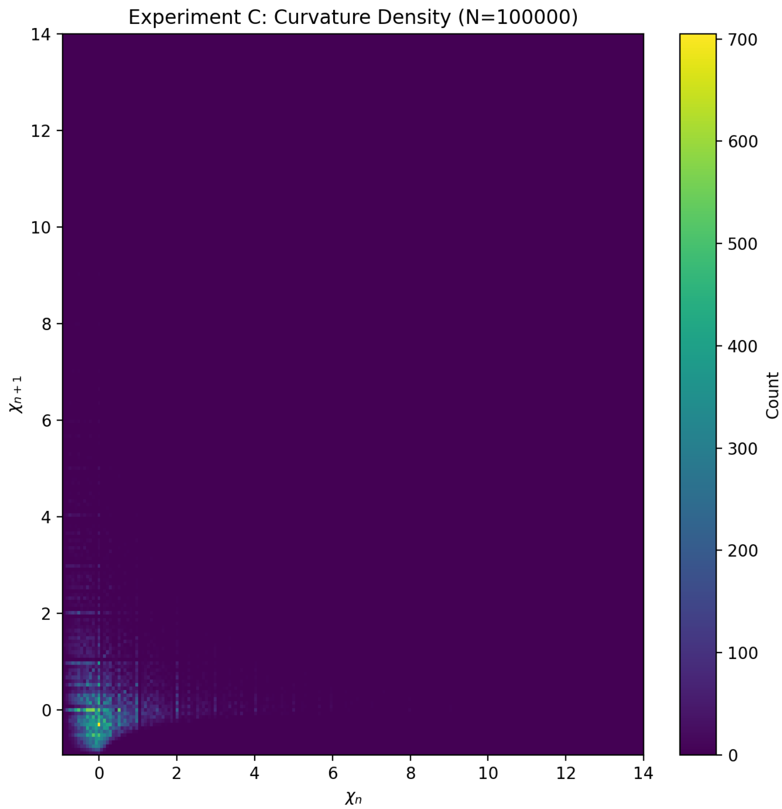

Figure 5: Experiment C: Density heatmap of (χ_n, χ_{n+1}) for $N = 100{,}000$. The bright core indicates strong concentration near $(0, 0)$, with smooth decay toward the boundary. No secondary clusters or lobes appear, confirming the attractor's geometric unity.

10 Experiment D: Multi-Scale Curvature Persistence

10.1 Smoothed Curvature Plots

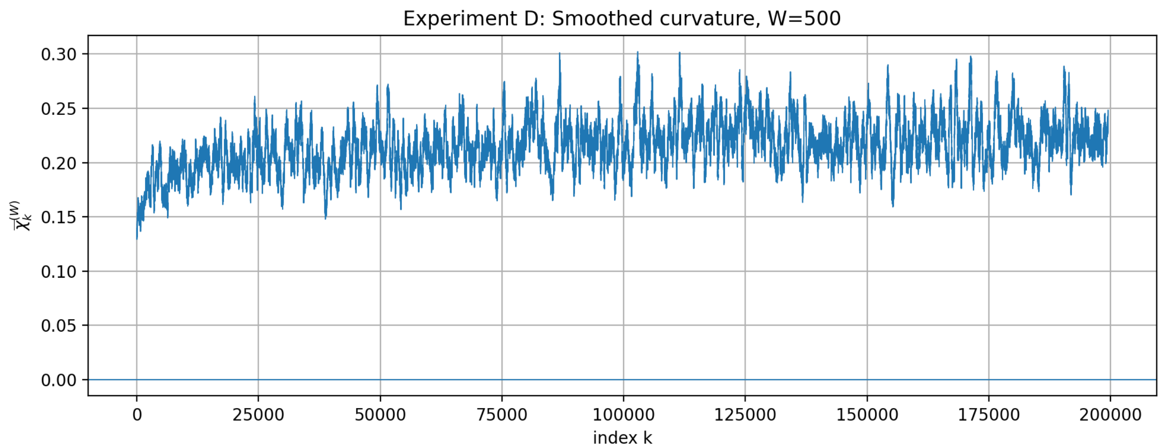

Figure 6: Experiment D: Sliding-window curvature with $W = 500$. The smoothed curvature remains strictly positive for nearly all 200,000 steps, forming a single coherent curvature phase. Random models do not exhibit such long-range sign stability.

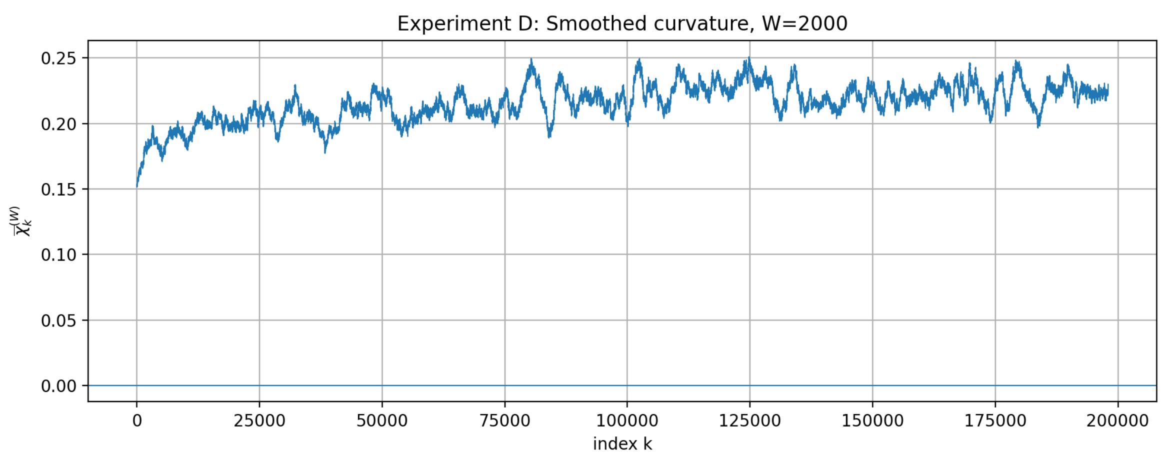

Figure 7: Experiment D: Smoothed curvature with $W = 2000$. The positive curvature phase persists across the entire dataset, even at this large smoothing scale. This indicates a deep global structure in the gap dynamics.

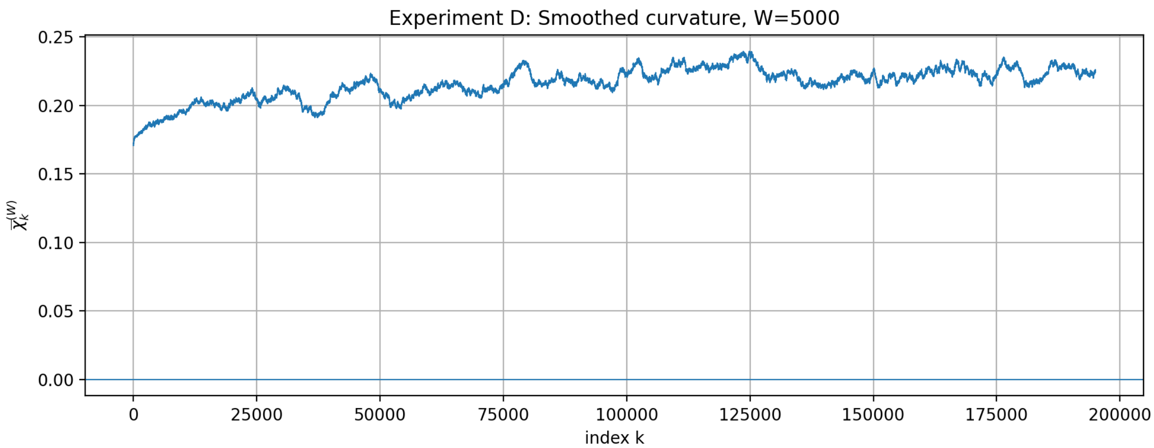

Figure 8: Experiment D: Smoothed curvature with $W = 5000$. The single positive phase remains unbroken, showing remarkable long-range coherence.

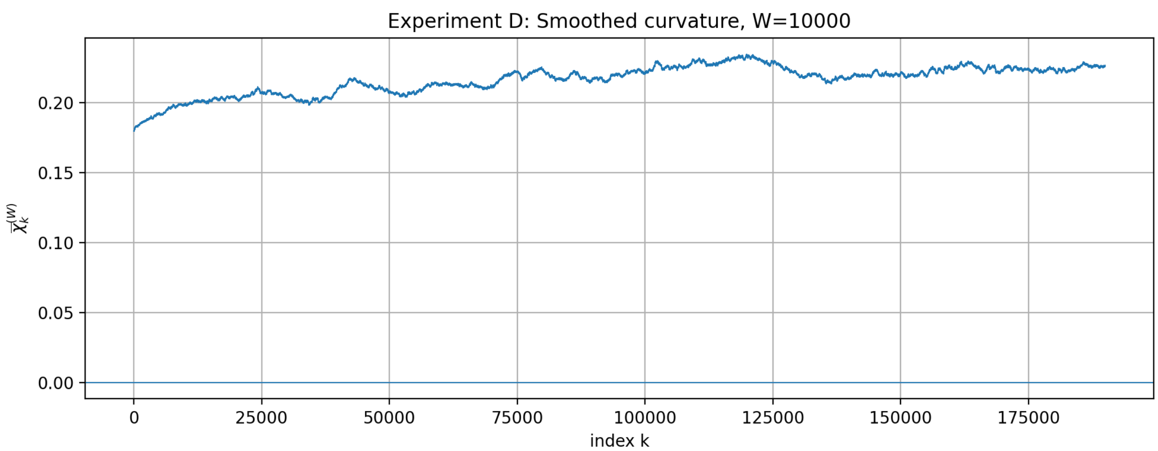

Figure 9: Experiment D: Smoothed curvature with $W = 10000$. Even with heavy smoothing, the curvature never crosses zero. This reveals a global curvature "season" extending over almost the entire range of primes tested.

10.2 Run Length Distributions

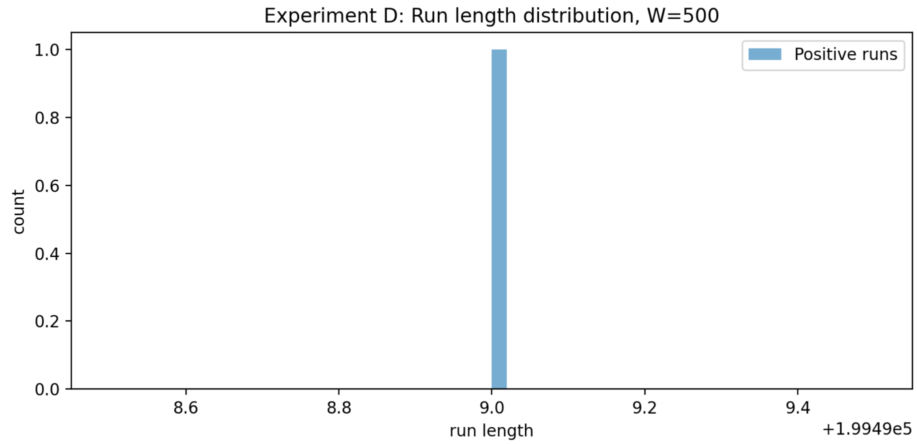

Figure 10: Histogram of positive and negative run lengths for $W = 500$. Only a single positive run exists (length 199,499); no negative runs occur. This supports the existence of a large-scale curvature phase.

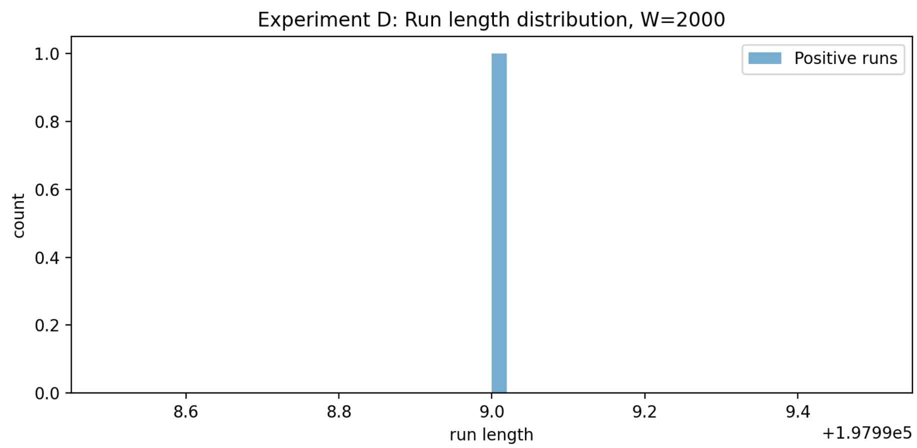

Figure 11: Run length distribution for $W = 2000$. Again, there is a single positive run and no negative runs, demonstrating large-scale coherence in the curvature sequence.

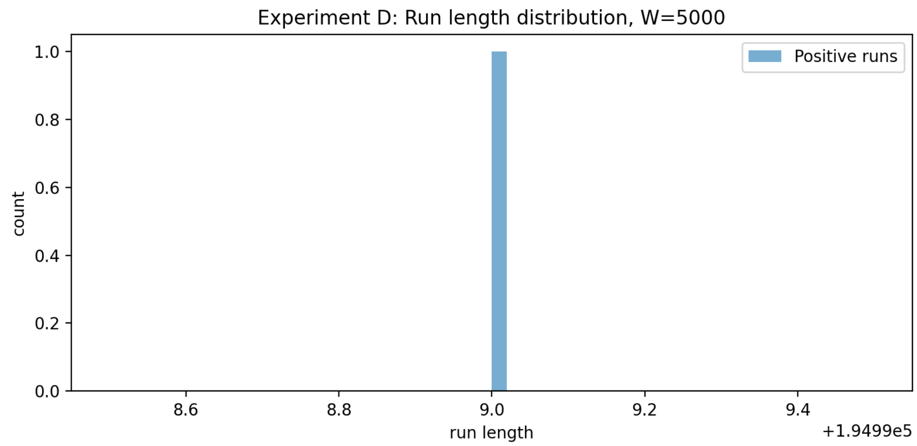

Figure 12: Run length distribution for $W = 5000$. The single positive run persists at this larger smoothing scale.

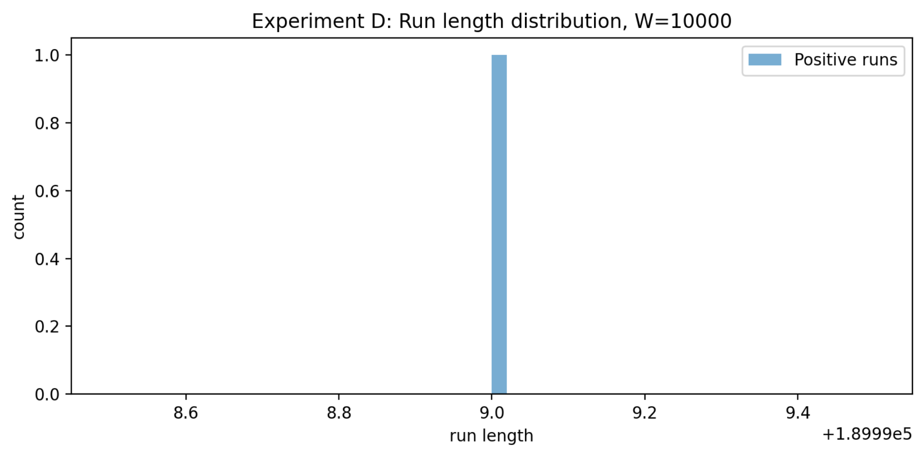

Figure 13: Run length distribution for $W = 10000$. The curvature dynamics remain in a single-phase region, with no sign reversals across the full dataset.

11 Conclusion

Prime Geometry III completes the synthesis of the algebraic, geometric, and dynamical components first developed in PG1 and PG2. The Prime Triangle identity provides a natural geometric backbone, the normalized curvature χ_n captures the local dynamics of gap evolution, and the action functional $S = \sum_n \chi_n^2$ aggregates global behavior.

The experiments carried out in this paper demonstrate four key facts: (1) the true prime sequence systematically minimizes the action relative to alternative gap orderings; (2) small perturbations disrupt the curvature attractor despite negligible action changes; (3) the attractor itself is compact, nearly isotropic, and quantitatively well-characterized; and (4) the curvature sequence exhibits long-range sign coherence across multiple smoothing scales.

Together, these results reveal that the prime gap sequence possesses a hidden geometric and dynamical structure that is not predicted by probabilistic models alone. Prime Geometry offers a complementary viewpoint on prime gaps—one in which local curvature and global action jointly constrain how consecutive primes evolve. The framework developed across PG1–PG3 suggests that prime gaps do not wander freely but instead follow a highly organized, low-curvature path through gap space.

12 Future Directions

Although this paper establishes the core of the action–curvature theory, several natural extensions remain open. These include higher-order action formulations, geometric structures for longer blocks of consecutive primes, analytic models that incorporate curvature suppression, and possible spectral interpretations involving the zeros of $\zeta(s)$. Large-scale experiments beyond 10^6 primes may further refine the attractor geometry and the scaling of the action gap. These directions will be pursued in future work (PG4 and beyond).

Acknowledgements

The conceptual development of Prime Geometry was shaped by extensive exploration, numerical experimentation, and iterative refinement across the PG1–PG3 series, with support from modern Artificial Intelligence resources. The author also acknowledges the open-source computational tools `primesieve`, `NumPy`, and `Matplotlib`, which made large-scale experimentation routine.

References

1. Cramér, H. "On the Order of Magnitude of the Difference Between Consecutive Prime Numbers." *Acta Arithmetica* 2 (1936): 23–46.

2. Hardy, G. H., and Littlewood, J. E. "Some Problems of 'Partitio Numerorum' III: On the Expression of a Number as a Sum of Primes." *Acta Mathematica* 44 (1923): 1–70.

3. Odlyzko, A. M. "The 10^{20}-th Zero of the Riemann Zeta Function and 175 Million of Its Neighbors." Preprint (1989).

4. Oliveira e Silva, T., Herzog, S., and Pardi, S. "Empirical Verification of the Even Perfect Number Conjecture up to 4×10^{18}." (Context for large-scale prime computations.)

5. Ribenboim, P. *The Book of Prime Number Records*. Springer, 1988. (A legendary compendium of prime trivia and world-record prime facts; often described as "a phone book for numbers that no one actually phoned.")